Supporting Information

Degradation Mechanism of Ni-Rich Cathode Materials: Focusing on Particle Interior

Nam-Yung Park,[1] Geon-Tae Park,[1] Su-Bin Kim [1] Wangmo Jung,[2] Byung-Chun Park,[2] and Yang-Kook Sun[1,]*

[1] Department of Energy Engineering, Hanyang University, Seoul 04763, South Korea

[2] Battery R&D Center, LG Energy Solution Ltd., Daejeon 34122, South Korea

AUTHOR INFORMATION

Corresponding Authors

E-mail: Y.-K.S: yksun@hanyang.ac.kr (Y.-K.S.)

EXPERIMENTAL METHODS

Synthesis of Cathode Materials: Hydroxide precursors of $[Ni_xCo_yMn_{1-x-y}](OH)_2$ (x = 0.8 and 0.9) were synthesized by the coprecipitation method in a batch reactor under a N_2 atmosphere. A 2.0 M aqueous transition metal (TM) solution was prepared by dissolving $NiSO_4 \cdot 6H_2O$, $CoSO_4 \cdot 7H_2O$, and $MnSO_4 \cdot H_2O$ (Samchun Chemicals) according to their final composition and fed into the reactor with NaOH (aq.) (Samchun Chemicals) and NH_4OH (aq.) (Junsei Chemical Co.) solutions. The molar ratios of NaOH/TM and NH_4OH/TM were ~2.0 and ~1.2, respectively. After growing the spherical precursor particles to 10 μm, the synthesized precursor slurry was washed, filtered, and dried at 110 °C in a vacuum oven. To obtain the NCM811 and NCM90 cathodes, the $[Ni_xCo_yMn_{1-x-y}](OH)_2$ precursors were mixed with $LiOH \cdot H_2O$ (Sigma-Aldrich) at a Li:TM molar ratio of 1.01:1.00. The mixtures were calcined at 750 °C (NCM90) and 800 °C (NCM811) for 10 h in a furnace (Lindberg, Thermo Fisher) under an O_2 atmosphere.

Material Characterization: The atomic composition of the cathode powders was confirmed using ICP-OES (Optima 8300, PerkinElmer). The surface and cross-sectional morphologies of the cathode particles were analyzed by SEM (Verios, G4UC, FEI); the cross-sections of the particles were polished using a cooling cross-section polisher (IB-19520CCP, JEOL). The XRD patterns of the cathode materials were obtained using XRD (Empyrean, PANalytical) with Cu Kα radiation in the 2θ range of 10–130°. Using the FullProf Suite, the structural parameters were analyzed by Rietveld refinement. To investigate changes in the lattice parameters of the cathodes during charging, in situ XRD measurements were performed using the same equipment. These XRD patterns were recorded every 40 min in transmission mode, using pouch-type cells with a constant current of 0.05 C. For the post-mortem analyses of cathodes after cycling, the electrodes were recovered from disassembled cells in an Ar-filled glove box. For TEM (NEO ARM, JEOL)

and TEM-EDS (Talos F200X, Thermo Fisher Scientific) analyses, cathode particle samples were prepared using a FIB (JEM-2100F, JEOL). Depth profiling and 3D rendering images for the TOF-SIMS (TOF.SIMS-5, ION-TOF) analysis were performed in the negative mode with an etching source of Cs^+ (500 eV, 40 nA). The SSRM mode of AFM (XE-200, Park Systems) was conducted in the range of 10 pA to 100 mA with a spatial resolution of <20 nm. The diamond-coated tips (CDT-NCHR, Park Systems) scanned the cross-sections of the electrodes at a bias of 3 V, detecting the current using a logarithmic current amplifier.

Electrochemical Tests: The cathode electrodes were fabricated by mixing the cathode powders with KS-6 graphite, Super-P (carbon black), and polyvinylidene fluoride (PVDF) with N-methyl-2-pyrrolidone in a dry room. The weight ratios of the cathode:KS-6:Super-P:PVDF were 90:3.3:2.2:4.5 for half-cell tests and 94:1.8:1.2:3 for the full-cell tests. The cathode slurry was coated on Al foil using a doctor blade and dried under vacuum at 110°C. The dried electrodes were then pressed with a load of 3.5 kN using a roll-press machine and punched with a diameter of 14 mm for coin cells and 3 × 5 cm^2 for pouch cells (the loading level of the active materials was 4 and 10 $mg \cdot cm^{-2}$ for half- and full-cells, respectively). Half-cells were assembled using 2032 coin-type cell parts (Hohsen) with the prepared cathode, separators (Celgard 2320, Celgard), Li-metal anodes (Honjo Metal, diameter = 16 mm, thickness = 400 μm), and an electrolyte (1.2 mol L^{-1} $LiPF_6$ in ethylene carbonate–ethyl methyl carbonate in a 3:7 volume ratio with 2 wt% vinylene carbonate, Panax Etec). Full-cells were assembled using pouch-type bi-cells featuring the prepared cathode, separator, electrolyte, and a graphite anode coated on Cu foil (ENERTECH) with an N/P ratio of 1.2 (cell capacity: 60 mAh, areal capacity: 2 mAh cm^{-2}). Electrochemical tests of half-cells were performed using a battery test system (TOSCAT-3100U, Toyo system) at 30 °C in the voltage range of 2.7–4.3 V. Cycling tests of the half-cells were

conducted under a constant current of 0.5C (90 mA g^{-1}). The rate capability was tested by sequentially increasing the discharge current (0.2C–0.5C–1.0C–2.0C–5.0C) with a fixed charge current of 0.2C. GITT was performed by repeatedly applying 0.05C current for 10 min and resting for 20 min. Electrochemical impedance spectroscopy was performed on the fresh and cycled cathodes after charging the half-cells to 4.3 V with a potentiostat (Bio-Logic, VMP3) from 1 MHz to 1 mHz. Long-term cycling tests using full-cells were conducted at 25 °C in the voltage range of 3.0–4.2 V using the same test equipment with a constant current of 0.8C (144 mA g^{-1}) for charge and 1.0C (180 mA g^{-1}) for discharge. Before and after 1000 cycles, in situ XRD and HPPC tests were performed (the test method for the latter is described in the battery test manual for EVs[1]).

(1) Battery test manual for electric vehicles revision 3, Idaho National Lab. (INL), June 1, 2 015; https://doi.org/10.2172/1186745 (accessed: June 2022).

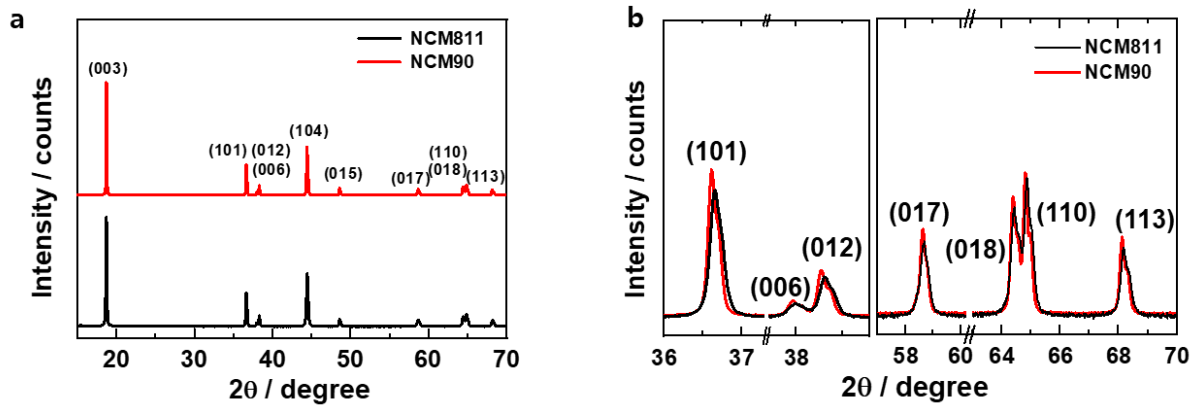

Figure S1. X-ray diffraction (XRD) patterns of the as-prepared NCM811 and NCM90 cathodes.

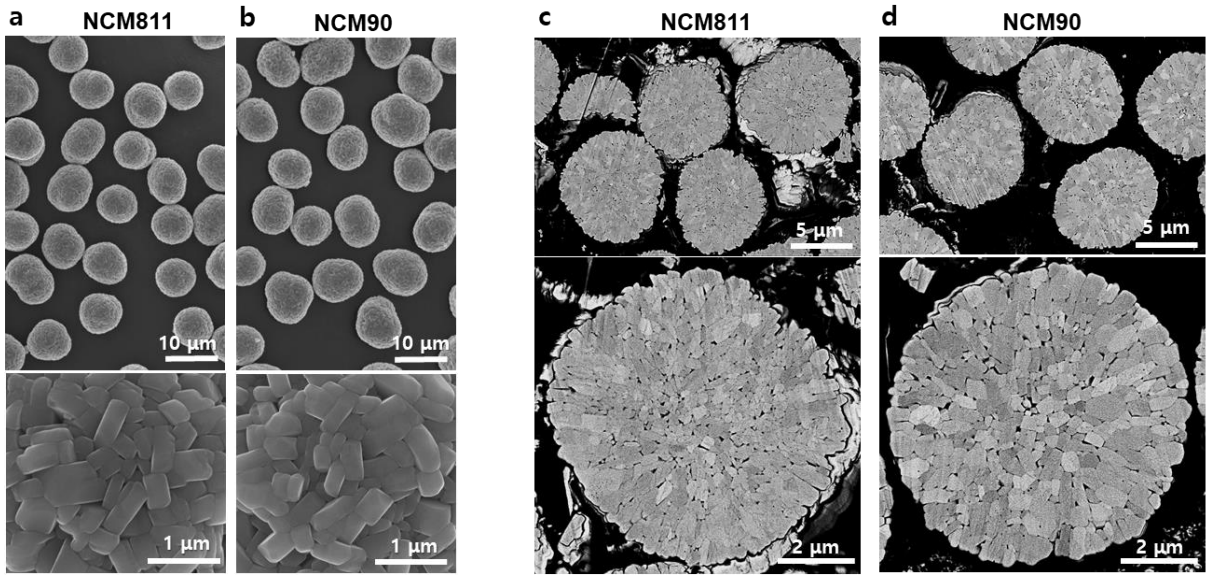

Figure S2. Scanning electron microscopy (SEM) images of (a) NCM811 and (b) NCM90 cathodes. Cross-sectional SEM images of (c) NCM811 and (d) NCM90 cathodes.

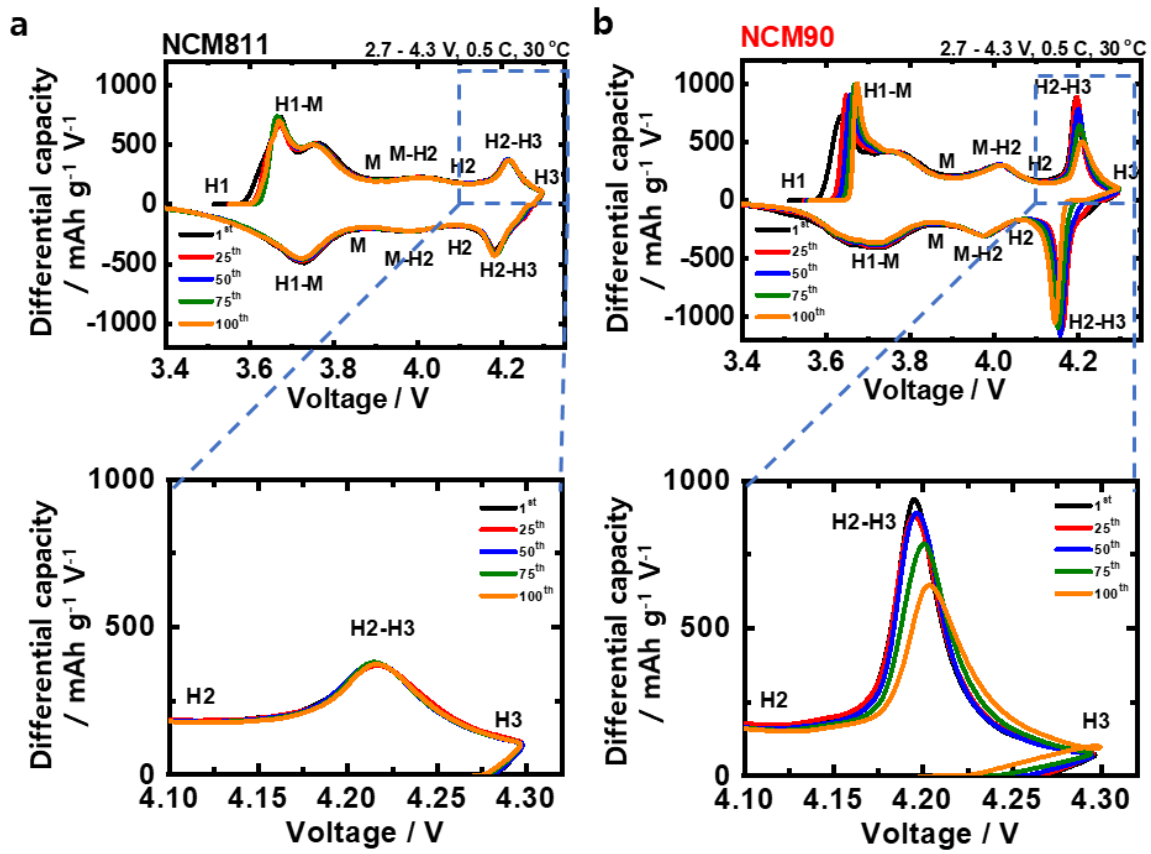

Figure S3. Differential capacity (dQ dV^{-1}) curves and magnified redox peaks of the H2–H3 phase transition of cells featuring (a) NCM811 and (b) NCM90 at the 1st, 25th, 50th, 75th, and 100th cycles.

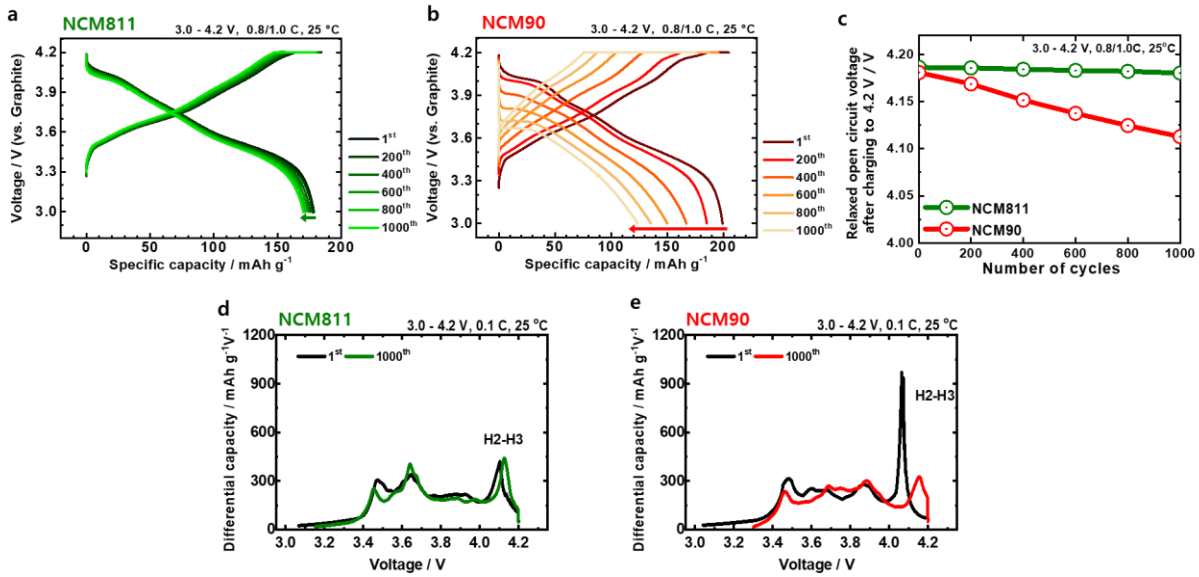

Figure S4. (a) Charge–discharge curves of full-cells featuring (a) NCM811 and (b) NCM90 cathodes cycled between 3.0 V and 4.2 V at 0.8/1.0C at 25 °C using a graphite anode plotted every 200 cycles. (c) Relaxed open circuit voltage after charging to 4.2 V for the full-cells featuring NCM811 and NCM90 cathodes plotted every 200 cycles. dQ dV^{-1} curves for the (d) NCM811, (e) NCM90 cathodes at the 1st and 1000th cycles.

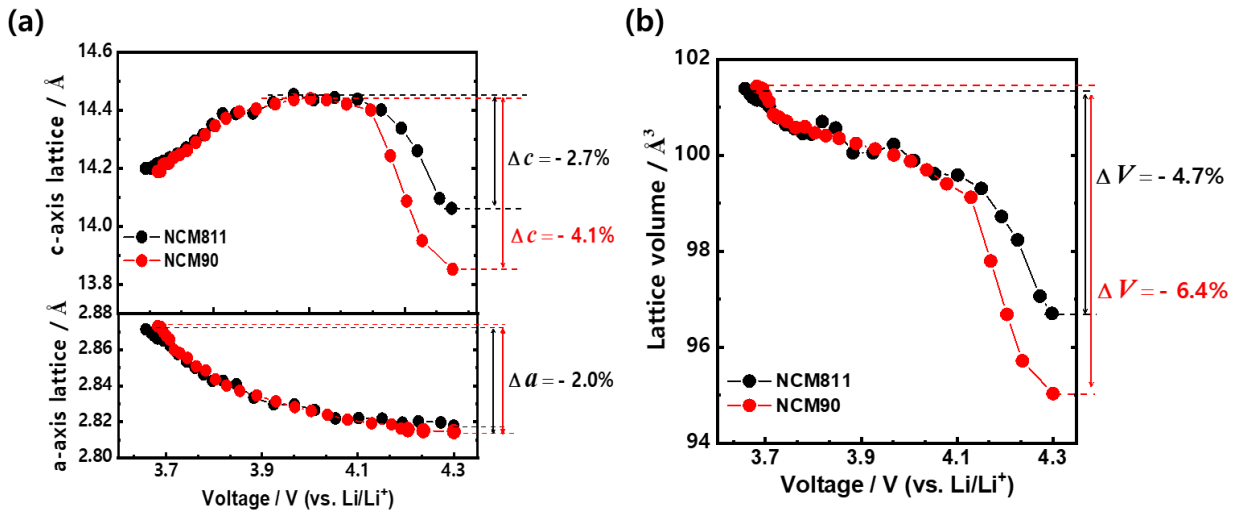

Figure S5. Changes in (a) lattice parameters (c-axis and a-axis) and (b) lattice volume in the NCM811 and NCM90 cathodes during charging, obtained from in situ XRD data.

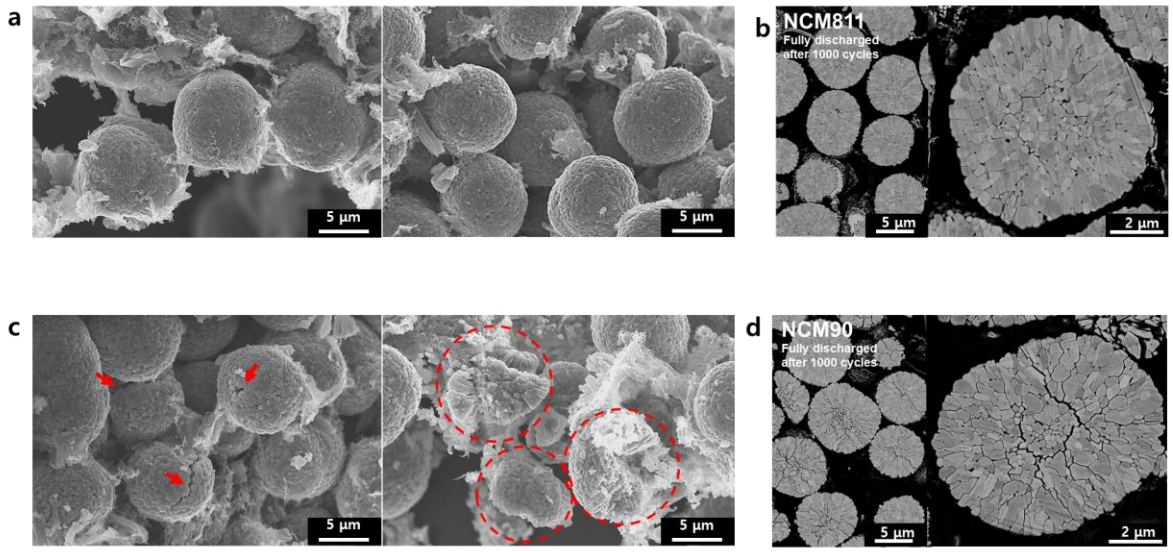

Figure S6. SEM images and cross-sectional SEM images of (a), (b) NCM811 and (c), (d) NCM90 cathodes fully discharged to 2.7 V after 1000 cycles.

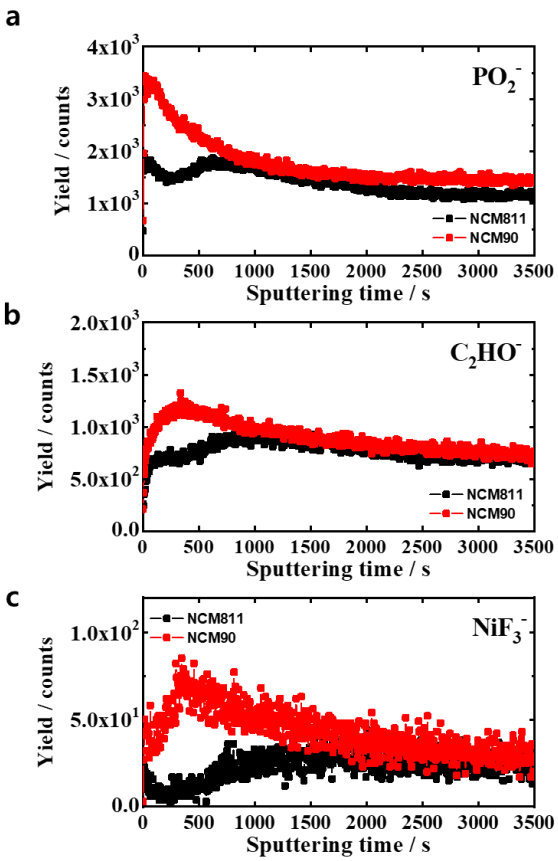

Figure S7. TOF-SIMS depth profiling of $PO2^-$, C_2HO^-, and $NiF3^-$ species in the NCM811 and NCM90 electrodes after 1000 cycles.

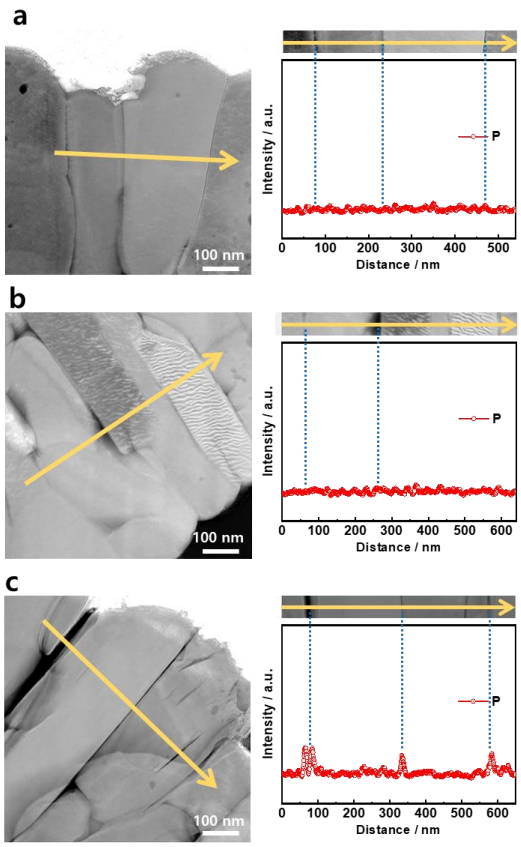

Figure S8. TEM-EDS line scans of P across the grain boundaries of (a), (b) NCM811 and (c) NCM90 cathodes after 1000 cycles.

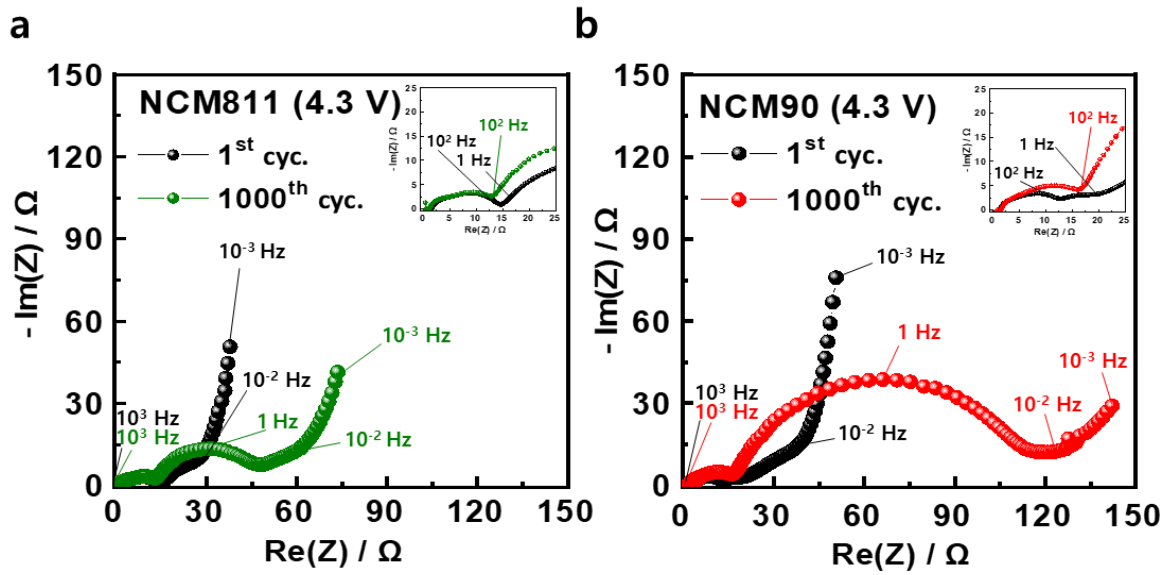

Figure S9. Comparison of the Nyquist plots of the measured electrochemical impedances (1 MHz–1 mHz) of (a) NCM811 and (b) NCM90 cathodes, charged to 4.3 V (vs. Li^+/Li) before and after 1000 cycles.

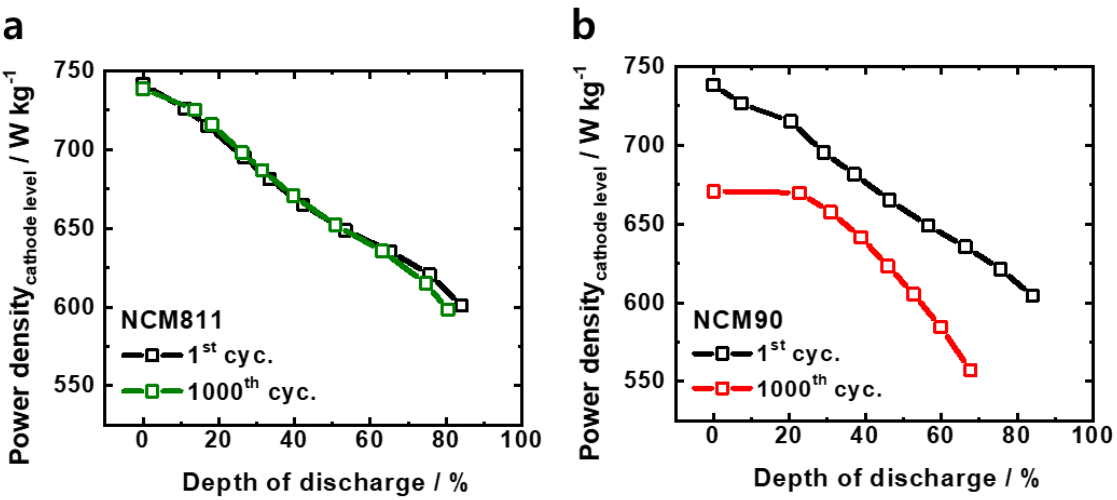

Figure S10. Power capability of the (a) NCM811 and (b) NCM90 cathodes as functions of the DoD before and after 1000 cycles.

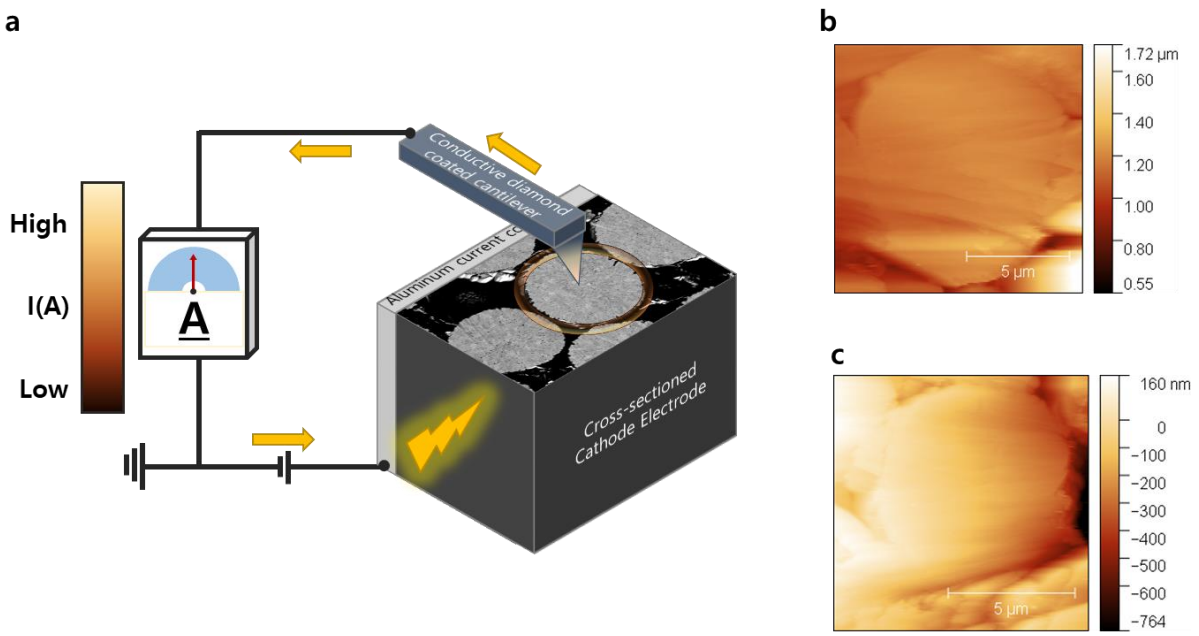

Figure S11. (a) Schematic image of the scanning spreading resistance microscopy (SSRM) measurement system used in AFM. SSRM topography images from cross-sections of (b) NCM811 and (c) NCM90 cathodes charged to 4.3 V (vs. Li^+/Li) after 1000 cycles.

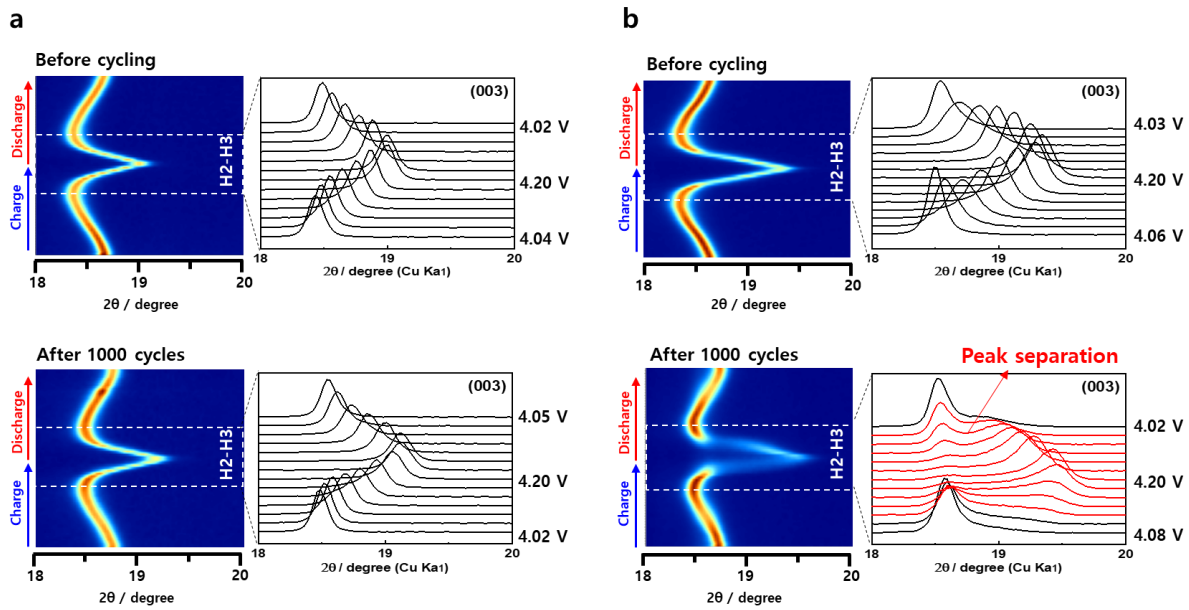

Figure S12. Contour plots of the (003) reflections of (a) NCM811 and (b) NCM90 cathodes measured before and after 1000 cycles.

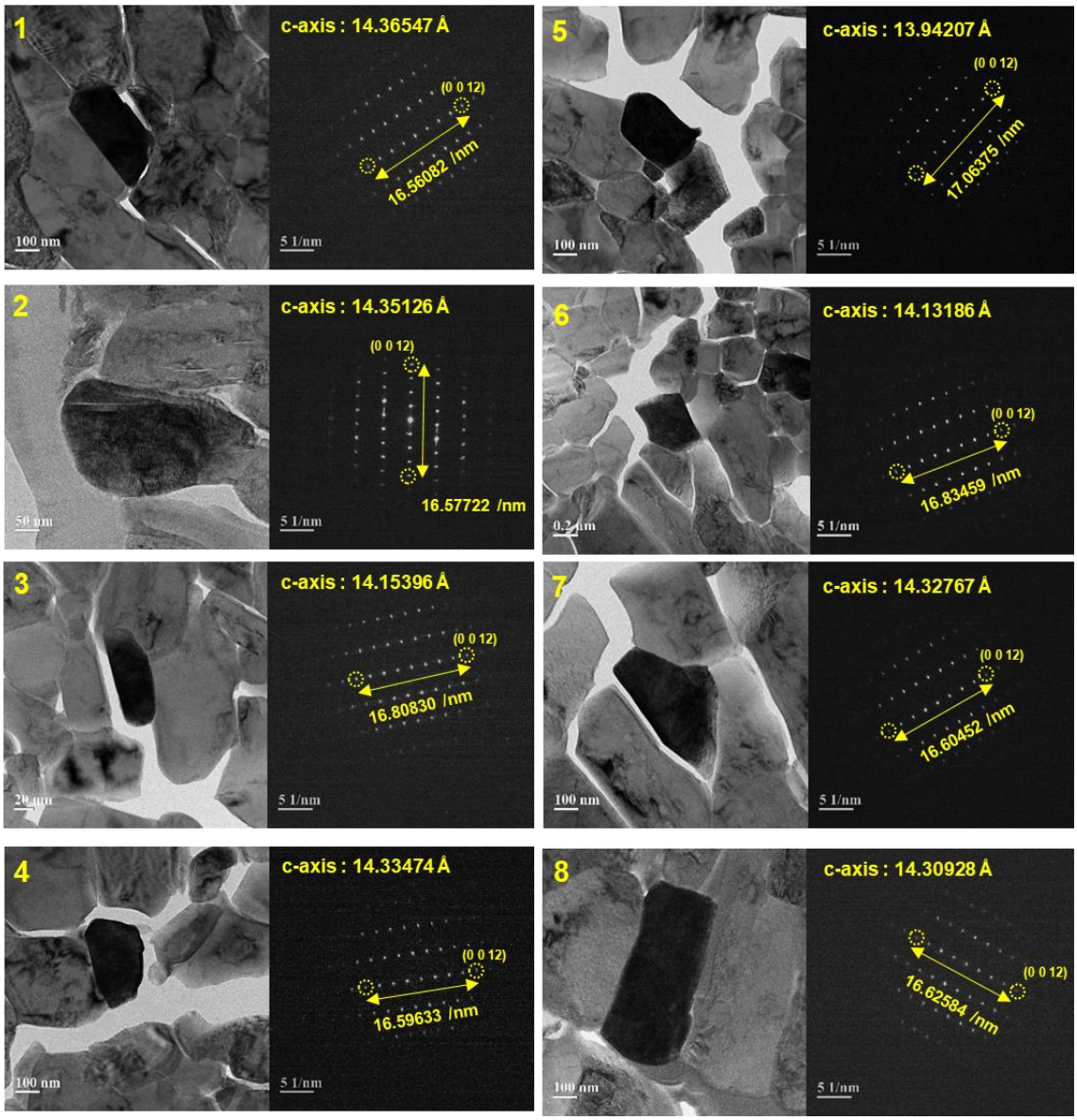

Figure S13. Selected-area electron diffraction (SAED) patterns from the regions marked in Figure 5c.

Table S1. Chemical compositions of the cathode materials determined by ICP-OES.

Sample	ICP-OES results (at%)		
	Ni	**Co**	**Mn**
NCM811	79.9	10.3	9.8
NCM90	89.9	5.3	4.8

Table S2. Structural parameters of NCM811 and NCM90 cathodes, as determined by the Rietveld refinement of the associated XRD data.

Sample	a_{hex} (Å)	c_{hex} (Å)	V (Å^3)	Ni^{2+} in Li layer (%)
NCM811	2.87221	14.20990	101.5206	2.2
NCM90	2.87328	14.20194	101.5393	1.7

Table S3. Checklist of experimental details in this work.

	Confirmed	N/A	Additional comments
Battery assembly			
Design of cell structure (e.g., 2032-coin cell, 3 cm * 5 cm pouch type cell, or others)	✓		In Experimental Methods
The relative weights of the active materials, conducting agent, and binder in an electrode	✓		
The loading level of the active material (mg/cm^2) in the electrode	✓		
The capacity balance between the cathode and anode (N/P) in a full cell	✓		
Lithium metal thickness and size (lithium metal cells)	✓		
Composition of electrolyte and details of additives	✓		
The amount the electrolyte and the ratio of electrolyte to active material.	✓		
Specifications of used materials (amount in grams, purity, concentration, vendor, etc.)	✓		
Evaluation of electrochemical performance			
Type of cell (half or full cells) used for the electrochemical tests	✓		In caption of Figure 1
Number of the stacked electrodes and the corresponding total capacity (full cells)	✓		In Experimental Methods
Cell capacity (mAh) or areal capacity (mAh/cm^2)	✓		
Theoretical capacity to determine C-rate and C-rate for each electrochemical test	✓		
The range of the operating voltage	✓		
The ambient temperature during electrochemical evaluations	✓		
Specified C-rate for each electrochemical	✓		

test			
First cycle or initial pre-cycling conditions and electrochemical data	✓		In Figure 1
Initial charge–discharge Ah efficiency and the capacity evaluated at a low C-rate (e.g., 0.1 C)	✓		
Pressure applied to the cell (if additional pressure is applied during cycling)		✗	The pouch-type full cells were tested without additional pressure.
Method of calculation of energy density (material, electrode, cell, pack level, etc.)		✗	Not applicable
Electrochemical testing procedures and CC/CV mode	✓		In Experimental Methods